Journal of Marine Science and Technology

Volume 22 | Issue 6 Article 10

PERIODIC DAMAGE EVALUATION OF AGING OFFSHORE JACKETS BASED ON CONTINUOUS DYNAMIC TESTS

Fu-Shun Liu
Department of Ocean Engineering, Ocean University of China, Qingdao, China, percyliu@ouc.edu.cn

Hong-Chao Lu
Department of Ocean Engineering, Ocean University of China, Qingdao, China.

Wei-Ying Wang
Center for Engineering Test and Appraisal, Qingdao Technological University, Qingdao, China

Dong-Ping Yang
Technology Inspection Center, China Petroleum & Chemical Corporation, Dongying, China

PERIODIC DAMAGE EVALUATION OF AGING OFFSHORE JACKETS BASED ON CONTINUOUS DYNAMIC TESTS

Acknowledgements

This research work is financially supported by the 973 project (Grant no. 2011CB013704) of the National Natural Science Foundation of China (Grant nos. 51279188, 51009124, 51379197, 51479184).

Journal of Marine Science and Technology, Vol. 22, No. 6, pp. 732-738 (2014)
DOI: 10.6119/JMST-014-0321-10

PERIODIC DAMAGE EVALUATION OF AGING OFFSHORE JACKETS BASED ON CONTINUOUS DYNAMIC TESTS

Fu-Shun Liu[1], Hong-Chao Lu[1], Wei-Ying Wang[2], and Dong-Ping Yang[3]

Key words: periodically evaluation, damage, platform, dynamic test.

ABSTRACT

This study proposes a new method for evaluating the damage of aging offshore platforms, based on dynamic tests. The proposed method involves a new damage indicator for reducing the effects of occurred damages accumulated before the first measurement. One theoretical improvement is that the requirement of using the stiffness matrix of the finite element model to replace that of the measured model can be ignored in calculating the modal strain energy of the measured model. The other development is that the proposed approach can be used for providing reasonable evaluations of damages that occurred between two adjacent dynamic tests. This improvement is crucial for evaluating aging platforms because such platforms have seldom been tested for damage detection during their previous service life. For demonstrating the applicability of the proposed method, numerical studies were conducted for a 3D offshore platform based on data generated from finite element models. The results indicated that the proposed method can be used to identify accurately the damages that occurred between the two measurements and to provide an accurate estimation of damage severity.

I. INTRODUCTION

In China, more than 300 fixed offshore platforms have been constructed. Approximately 200 of these platforms belong to the China National Offshore Oil Corporation, and more than 100 platforms belong to the China Petrochemical Corporation. According to the statistics of the Offshore Oil Engineering Co., LTD, this company's offshore platforms that served for less than 5 years comprise 28% of their nearly 200 fixed platforms; furthermore, those that served for 5-10, 10-20, and more than 20 years comprise 26%, 29%, and 17% of their approximate 200 fixed platforms. Such marine structures require proper maintenance to ensure the safety of their operation, especially for those that have been used for more than 10 years. The primary principle of maintaining an offshore structure is to ensure its safety and functional performance during its design service life. Damage detection methods can be used to inspect whether local damages have appeared and evaluate integrity of the structures for increasing their operational lifetime and improving safety.

Numerous studies have investigated the damage detection of jacket-type offshore structures [9, 13]. Elshafey *et al*. [1] examined damage detection in offshore jacket platforms by using a combined method involving random decrement signature and neural networks. Shi *et al*. [11] proposed using the change of modal strain energy (MSE) in each element as a damage indicator; the process was proven to be effective in locating structural damages. However, because these damaged elements were unknown, the damaged elemental stiffness matrix was replaced by the undamaged for an approximation in calculating the MSE change of the nth element for the jth mode. The modal strain energy decomposition (MSED) method was developed by Li *et al*. [4] for 3D frame structures, which is used to define two damage indicators: the axial damage indicator and transverse damage indicator, for each member. The accuracy of localizing damage elements is improved considerably by analyzing the joint information of two damage indicators. However, the MSED method cannot be used to achieve satisfactory estimates of damage severity. Li *et al*. [3] extended the cross-model cross-mode method CMCM method to damped systems for damage detection by using spatially incomplete complex modes. The effectiveness of the method was demonstrated using a cantilever beam structure, which was employed by Friswell *et al*. [2]. However, additional studies have indicated the method was sensitive to noise. Mojtahedi *et al*. [10] experimentally investigated a laboratory model of a jacket platform for establishing a baseline finite element (FE) model for long-term structural health

Paper submitted 08/25/13; revised 01/10/14; accepted 03/21/14. Author for correspondence: Fu-Shun Liu (e-mail: percyliu@ouc.edu.cn).
[1] Department of Ocean Engineering, Ocean University of China, Qingdao, China.
[2] Center for Engineering Test and Appraisal, Qingdao Technological University, Qingdao, China.
[3] Technology Inspection Center, China Petroleum & Chemical Corporation, Dongying, China.

monitoring of offshore structures.

Liu [5] presented a direct estimation method for expanding incomplete experimental mode shapes and investigated its performance by using a 5-DOFs mass-spring system and a steel cantilever-beam experiment. Liu *et al*. [6, 7] presented a rapid mode shape expansion method without considering the modeling errors. In this method, no constraints are imposed; numerical studies indicated that the estimation of unmeasured mode shape components are influenced when modeling errors exceed the limitation of the method. Liu and Li [8] discussed applying an iterative expansion method to offshore platforms.

In the current study, a numerical offshore platform was used to demonstrate the applicability of the proposed method, including spatial incomplete situations. A scale model of an offshore structure was used as for evaluating the efficiency of the proposed approach.

II. PERIODIC DAMAGE EVALUATION

For an nth element, the MSE of the *i* th mode for the baseline model $\mathbf{\Phi}_i$ and *j* th mode for the measured model $\mathbf{\Phi}_j'$ can be calculated as follows:

$$MSE_{ni} = \left(\mathbf{\Phi}_i\right)^t \mathbf{K}_n \mathbf{\Phi}_i \tag{1}$$

$$MSE'_{nj} = \left(\mathbf{\Phi}_j'\right)^t \mathbf{K}_n' \mathbf{\Phi}_j' \tag{2}$$

where $\mathbf{K}_n$ and $\mathbf{K}_n'$ represent a preselected stiffness submatrix of the baseline model and measured model, respectively. Furthermore, the stiffness submatrix $\mathbf{K}_n'$ of the measured model is a modification of $\mathbf{K}_n$:

$$\mathbf{K}_n' = \mathbf{K}_n + \alpha_n \mathbf{K}_n \tag{3}$$

where α_n are unknown stiffness correction factors that must be determined; when the structure is first tested, Eq. (6) can be written as follows:

$$MSE'_{nj,rf} = \left(\mathbf{\Phi}'_{j,rf}\right)^t \mathbf{K}'_{n,rf} \mathbf{\Phi}'_{j,rf} \tag{4}$$

when the MSE for several modes are considered collectively, the MSE_n, $MSE'_{n,rf}$, and $MSE'_{n,rp}$ of the nth element is defined as the average of the sum of MSE_{ni}, $MSE'_{nj,rf}$, and $MSE'_{nj,rp}$, respectively, as follows:

$$MSE_n = \frac{1}{Ni}\sum_{i=1}^{Ni} MSE_{ni} = \frac{1}{Ni}\sum_{i=1}^{Ni}\left(\mathbf{\Phi}_i\right)^t \mathbf{K}_n \mathbf{\Phi}_i \tag{5}$$

$$MSE'_{n,rf} = \frac{1}{N_{j,rf}}\sum_{j=1}^{N_{j,rf}} MSE'_{nj,rf}$$

$$= \frac{1}{N_{j,rf}}\sum_{j=1}^{N_{j,rf}}\left(\mathbf{\Phi}'_{j,rf}\right)^t \left(\mathbf{K}_n + \alpha_{n,rf}\mathbf{K}_n\right)\mathbf{\Phi}'_{j,rf} \tag{6}$$

$$MSE'_{n,rp} = \frac{1}{N_{j,rp}}\sum_{j=1}^{N_{j,rp}} MSE'_{nj,rp}$$

$$= \frac{1}{N_{j,rp}}\sum_{j=1}^{N_{j,rp}}\left(\mathbf{\Phi}'_{j,rp}\right)^t \left(\mathbf{K}_n + \alpha_{n,rp}\mathbf{K}_n\right)\mathbf{\Phi}'_{j,rp} \tag{7}$$

where Ni, $N_{j,rf}$, and $N_{j,rp}$ denote modes that are derived from the baseline model and measured model, respectively.

The corresponding expression for the MSEC of the nth element between the measured model at the second test moment and FEM can also be expressed as follows:

$$MSEC_{n,rp} = \frac{1}{N_{j,rp}}\sum_{j=1}^{N_{j,rp}}\left(\mathbf{\Phi}'_{j,rp}\right)^t \mathbf{K}_n \mathbf{\Phi}'_{j,rp}$$

$$+\frac{1}{N_{j,rp}}\sum_{j=1}^{N_{j,rp}} \alpha_{n,rp}\left(\mathbf{\Phi}'_{j,rp}\right)^t \mathbf{K}_n \mathbf{\Phi}'_{j,rp}$$

$$-\frac{1}{Ni}\sum_{i=1}^{N_i}\left(\mathbf{\Phi}_i\right)^t \mathbf{K}_n \mathbf{\Phi}_i \tag{8}$$

The MSEC of the nth element between the first and second tests of the measured model can be expressed as follows:

$$MSEC_n = \frac{1}{N_{j,rp}}\sum_{j=1}^{N_{j,rp}}\left(\mathbf{\Phi}'_{j,rp}\right)^t \mathbf{K}_n \mathbf{\Phi}'_{j,rp}$$

$$+\frac{1}{N_{j,rp}}\sum_{j=1}^{N_{j,rp}} \alpha_{n,rp}\left(\mathbf{\Phi}'_{j,rp}\right)^t \mathbf{K}_n \mathbf{\Phi}'_{j,rp}$$

$$-\frac{1}{N_{j,rf}}\sum_{j=1}^{N_{j,rf}}\left(\mathbf{\Phi}'_{j,rf}\right)^t \mathbf{K}_n \mathbf{\Phi}'_{j,rf}$$

$$-\frac{1}{N_{j,rf}}\sum_{j=1}^{N_{j,rf}} \alpha_{n,rf}\left(\mathbf{\Phi}'_{j,rf}\right)^t \mathbf{K}_n \mathbf{\Phi}'_{j,rf}. \tag{9}$$

The modal strain energy change ratio (MSECR) can also be a meaningful indicator for damage localization defined as follows:

$$D_{pf,n} = \frac{\frac{1}{N_{j,rp}}\sum_{j=1}^{N_{j,rp}} \alpha_{n,rp} \left(\boldsymbol{\Phi}'_{j,rp}\right)^t \mathbf{K}_n \boldsymbol{\Phi}'_{j,rp} - \frac{1}{N_{j,rf}}\sum_{j=1}^{N_{j,rf}} \alpha_{n,rf} \left(\boldsymbol{\Phi}'_{j,rf}\right)^t \mathbf{K}_n \boldsymbol{\Phi}'_{j,rf}}{\frac{1}{N_{j,rf}}\sum_{j=1}^{N_{j,rf}} \left(\boldsymbol{\Phi}'_{j,rf}\right)^t \left(\mathbf{K}_n + \alpha_{n,rf}\mathbf{K}_n\right)\boldsymbol{\Phi}'_{j,rf}}. \tag{10}$$

Based on the normalization procedure by Stubbs *et al*. [12], a new damage indicator of the nth element based on MSECR is defined as follows:

$$D_{pf,n} = \frac{D_{pf,n} - \overline{D_{pf,n}}}{\sigma_{D_{pf,n}}} \tag{11}$$

where $\overline{D_{pf,n}}$ and $\sigma_{D_{pf,n}}$ represent the sample mean and standard deviation of $D_{pf,n}$, respectively.

The relation for the j th eigenvalues and eigenvectors associated with $\mathbf{K}'$ and $\mathbf{M}'$ at the first test moment can be expressed as follows:

$$\mathbf{K}'\boldsymbol{\Phi}'_{j,rf} = \lambda'_{j,rf}\mathbf{M}'\boldsymbol{\Phi}'_{j,rf} \tag{12}$$

One obtains

$$\sum_{n=1}^{Ne} \alpha_{n,rf} \boldsymbol{\Phi}_i^T \mathbf{K}_n \boldsymbol{\Phi}'_{j,rf} = \lambda'_{j,rf} \boldsymbol{\Phi}_i^T \mathbf{M}\boldsymbol{\Phi}'_{j,rf} - \boldsymbol{\Phi}_i^T \mathbf{K}\boldsymbol{\Phi}'_{j,rf} \tag{13}$$

Eq. (13) can be rewritten in matrix form as follows:

$$\mathbf{S}_{rf,(Ni\times N_{j,rf})\times n}\boldsymbol{\Gamma}_{rf,(n\times 1)} = \mathbf{b}_{rf,(n\times 1)} \tag{14}$$

where

$$\mathbf{S}_{rf,(Ni\times N_{j,rf})\times n} = \boldsymbol{\Phi}_i^T \mathbf{K}_n \boldsymbol{\Phi}'_{j,rf} \tag{15}$$

$$\boldsymbol{\Gamma}_{rf,(n\times 1)} = \begin{Bmatrix} \alpha_{1,rf} \\ \alpha_{2,rf} \\ \vdots \\ \alpha_{n,rf} \end{Bmatrix} \tag{16}$$

$$\mathbf{b}_{rf,(n\times 1)} = \lambda'_{j,rf} \boldsymbol{\Phi}_i^T \mathbf{M}\boldsymbol{\Phi}'_{j,rf} - \boldsymbol{\Phi}_i^T \mathbf{K}\boldsymbol{\Phi}'_{j,rf} \tag{17}$$

A standard inverse operation can be used to solve for $\boldsymbol{\Gamma}$ in Eq. (27) as follows:

$$\boldsymbol{\Gamma}_{rf,n\times 1} = \left(\mathbf{S}_{rf,(Ni\times N_{j,rf})\times n}\right)^{-1} \mathbf{b}_{rf,n\times 1} \tag{18}$$

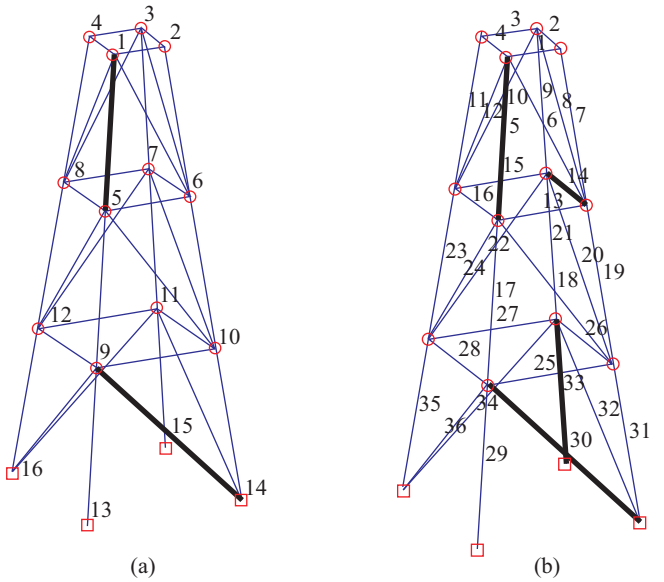

Fig. 1. Sketch of the offshore platform structure: (a) node numbering and (b) element numbering.

For resolving spatially incomplete situations, the direct mode shape expansion technique proposed by Liu [5] and Liu and Li [6-8] can be used to obtain spatially complete mode shapes as follows:

$$\mathbf{S}_{rf,(Ni\times N_{j,rf})\times n} = \boldsymbol{\Phi}_i^T \mathbf{K}_n \left(\boldsymbol{\Phi}'_{j,rf}\right)_D \tag{19}$$

where $\left(\boldsymbol{\Phi}'_{j,rf}\right)_D$ represents the spatially complete mode shape obtained by employing the direct mode shape expansion technique.

III. SIMULATION

In the numerical analysis, the applicability of the proposed method was evaluated using an offshore platform structure, as shown in Fig. 1. As shown in Fig. 1(a), an offshore structure was used as the test structure for demonstrating the proposed damage detection method. The structure, consisting of 36 steel tubular members with a uniform outer diameter (17.8 cm) and wall thickness (0.89 cm), was fixed to the ground. The heights of the three stories were all 9.14 m, and the side lengths of the floors, from first to fourth, were 10.97, 8.53, 6.10, and 3.66 m, respectively. The essential material properties of the steel tubular members were: elastic modulus E = 2.1 × 10^{11} N/m^2, linear mass density ρ = 7850 kg/m^3, and Poisson's ratio ν = 0.3. Fig. 1 illustrates the node and element numbering, respectively. Modal analysis was performed by developing a program in Matlab for deriving the modal frequencies and mode shapes. The first three modal frequencies were 6.95, 9.69, and 9.71 Hz, respectively.

Table 1. Comparison of frequencies (Hz).

Order	Finite Element Model	Damaged Model Correspongding to the First Test	Damaged Model Correspongding to the Second Test
1	6.95	6.89	6.61
2	6.96	9.63	9.47
3	9.71	9.70	9.67
4	14.36	14.04	14.01
5	16.82	16.30	16.25

IV. IMPLEMENTATION

In this study, the test structure was considered a damaged platform. Two damaged models were established to represent different degrees of damage at various test moments. Therefore, this study first assumed that the stiffness of elements 24 and 30 were reduced by 35% and 25%, respectively, from the analytical model to examine the damages accumulated before the first measurement of the platform. This study subsequently assumed that the damages in elements 14 and 33 occurred after the first measurement of the platform because of the elements' reduced stiffness (i.e., by 35% and 25%, respectively). The second test of this platform was implemented for identifying these damages. The damaged elements represent different types of structural members and are illustrated in Fig. 1; Table 1 shows a comparison of the first five frequencies. The following numerical study was conducted with the main objective of determining whether damages that occurred after the first measurement could be detected accurately.

The errors caused by neglecting the two terms mentioned in Eq. (10) were first evaluated. For simplicity, these two terms are defined as follows:

$$\Gamma_{rp} = \frac{1}{N_{j,rp}} \sum_{i=1}^{N_{j,rp}} \left(\boldsymbol{\Phi}'_{j,rp} \right)^t \mathbf{K}_n \boldsymbol{\Phi}'_{j,rp} \tag{20}$$

and

$$\Gamma_{rf} = \frac{1}{N_{j,rf}} \sum_{i=1}^{N_{j,rf}} \left(\boldsymbol{\Phi}'_{j,rf} \right)^t \mathbf{K}_n \boldsymbol{\Phi}'_{j,rf}, \tag{21}$$

respectively.

Fig. 2 shows a comparison of the results between Γ_{rp} and Γ_{rf} when $N_{j,rp} = N_{j,rf} = 3$, clearly indicating that Γ_{rp} and Γ_{rf} demonstrate close values, except for positions at elements 14 and 33, thus explaining this phenomenon because damages occurred in these four elements.

Before the first platform measurement, elements 24 and 30 were damaged, whereas the damages in elements 14 and 33 were assumed to have occurred after the first measurement. For identifying the damages in elements 14 and 33, the second measurement was implemented. When the first two modes

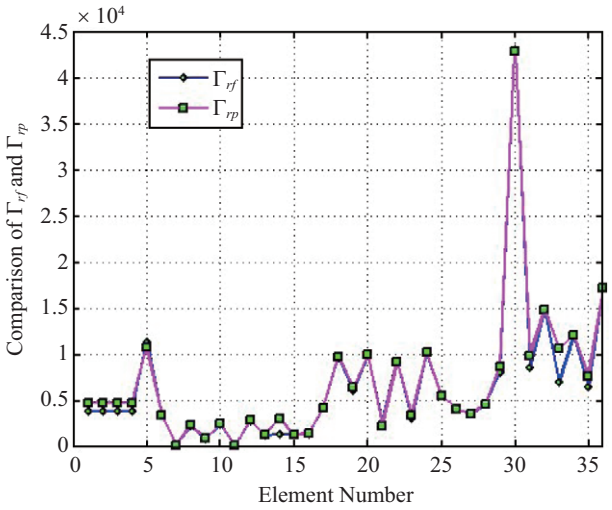

Fig. 2. Comparison between Γ_{rp} and Γ_{rf} when $N_{j,rp} = N_{j,rf} = 3$.

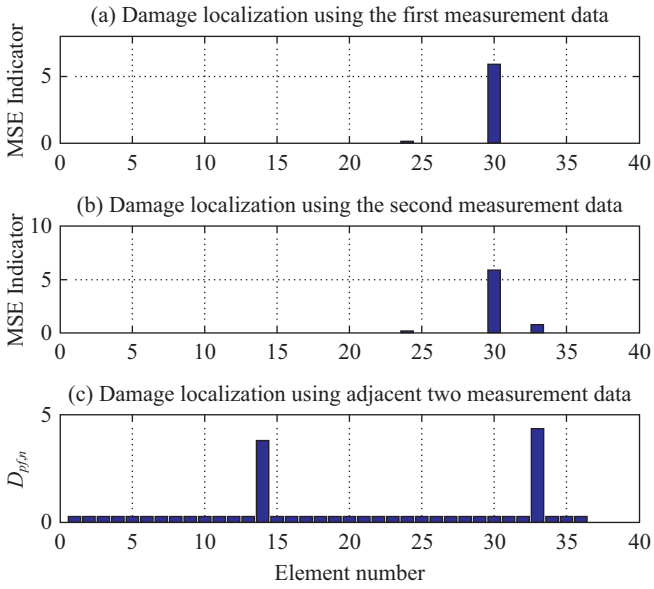

Fig. 3. Comparison of damage localization using the first and/or the second measurement data when only two damaged elements before the first measurement: (a) Damage localization using the first measurement data, (b) Damage localization using the second measurement data, and (c) Damage localization using adjacent two measurements data.

were obtained, the proposed method was implemented, and Fig. 3 shows the obtained results. Figs. 3(a) and (b) show the results of damage localization obtained using the first and second measurement data, respectively; Fig. 3(c) shows the damage localization results obtained by simultaneously using the first and second measurement data, respectively. This study concluded that the damage at element 30 could be detected using the first measurement, whereas the damage at element 14 was not so obvious. If only the second measurement is used, the damages at elements 30 and 33 could also be

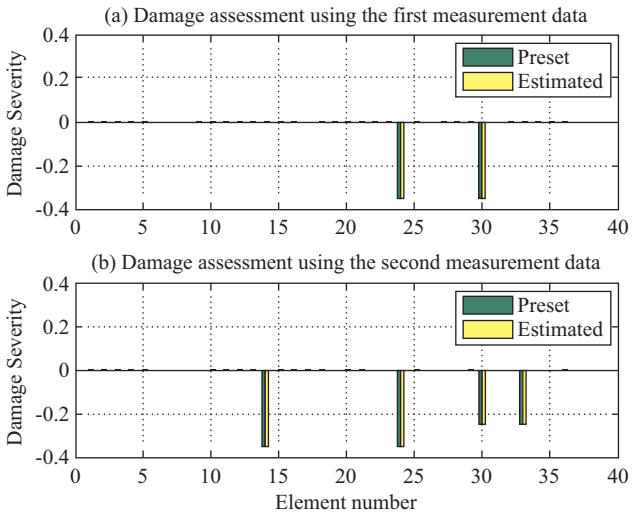

Fig. 4. Comparison of damage assessment using the first or the second measurement data when only two damaged elements before the first measurement: (a) Damage assessment using the first measurement data, and (b) Damage assessment using the second measurement data.

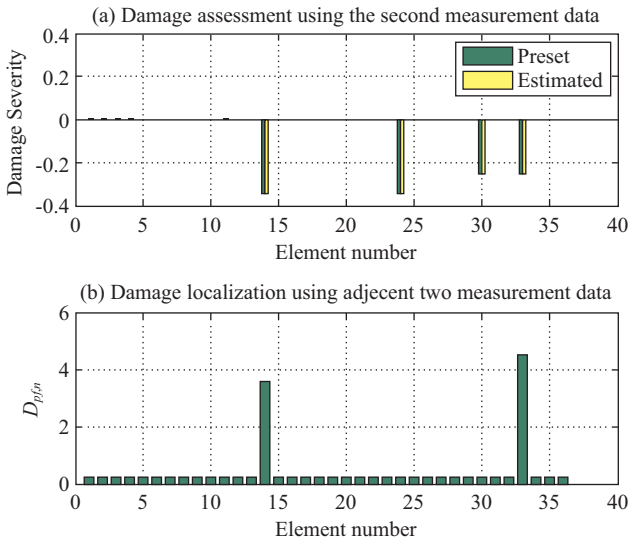

Fig. 5. Damage identification results when translational DOFs in x, y directions of nodes 1 to 12 are measured: (a) Damage assessment using the second measurement data, and (b) Damage localization using adjacent two measurement data.

identified. Fig. 4 shows the results of the damage severity estimation, indicating that the damages could be assessed accurately if the first three spatial complete modes are measured. Therefore, the damage deterioration that occurred between two adjacent measurements could be identified using the proposed method (Fig. 3(c)).

This study also determined whether the proposed method could accurately identify the damages when only the spatially incomplete modes are measured. This study assumed that only the translational degrees of freedom were measured for the first three modes at nodes 1 to 12 (shown in Fig. 1). Thus, 36 master degrees of freedom were measured. The proposed method was subsequently implemented, and Fig. 5 shows the obtained results, indicating that the damage locations were identified accurately when only the translational degrees of freedom in the x and y directions of the platform were measured; Fig. 5(a) illustrates the appropriate results of the damage severity estimation.

V. EXPERIMENTS

For evaluating the efficiency of the proposed approach, this study used a scale model of the real offshore structure. As shown in Fig. 6, the model has a scale factor of 1/15; this model is fabricated using steel tubes, with 34 × 3 mm sections for the three legs and vertical bracing and 20 × 2 mm sections for all braces. The numerical model shown in Fig. 7 represents the aforementioned physical model. The instruments consisted of 12 triaxial capacitive accelerometers (Model 4803A-0002) that were used for measuring the response, and a measurement system (PL64-DCB8, Integrated Measurement & Control Cooperation, Germany) that was used for data acquisition. The 12 triaxial capacitive accelerometers were

Fig. 6. The test model.

installed at nodes 4 to 6, and 10 to 18, and the model was excited by waves and currents in a water tank at Ocean University of China.

Two damage locations were examined in the structure; the first location was in the low slope bracing, and the second location was in the upper bracing (Fig. 7). Damages were modeled using two flanges, and the member was completely damaged by removing all the bolts in these flanges. The damaged member was restored to its original state by reinstalling the bolts. Fig. 8 shows the corresponding acceleration signals (Sensor 1) in the frequency domain, at a sampling rate of 500 Hz.

Before the first test, two flanges corresponding to elements 7 and 15 were fastened, and all bolts at element 7 were subsequently removed, and the first test was then conducted.

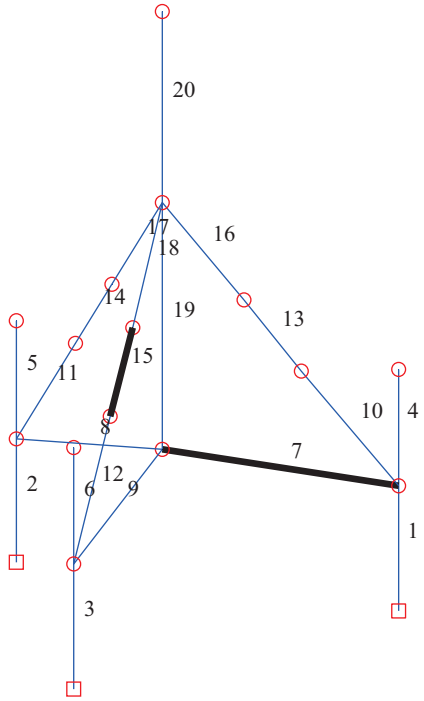

Fig. 7. Numerical model of the test structure.

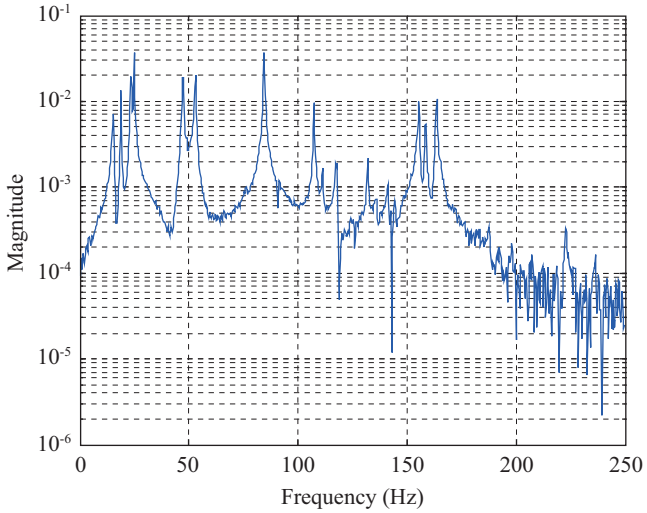

Fig. 8. Measured acceleration signal of Sensor 1 in frequency domain.

Fig. 9 shows the damage detection results obtained by implementing the proposed approach, indicating that damage at element 7 was identified accurately, and a damage severity estimation of -1.0661 was recorded. In addition, elements 15 and 18 also demonstrated some damages (Fig. 9). This is because the flange at element 15 was fastened inappropriately, implying that there were some damages at these two elements before the first dynamic test.

When the bolts at element 15 were removed completely before the second test, and when only the second measured data were applied to the proposed method, the results illus

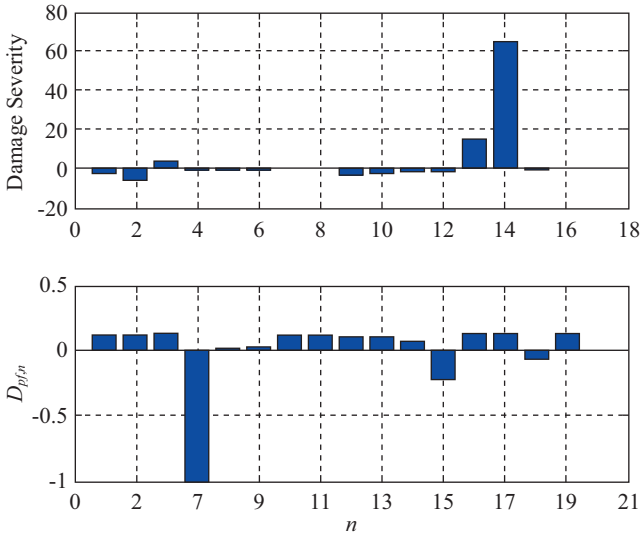

Fig. 9. Damage detection results when element 7 was cut off.

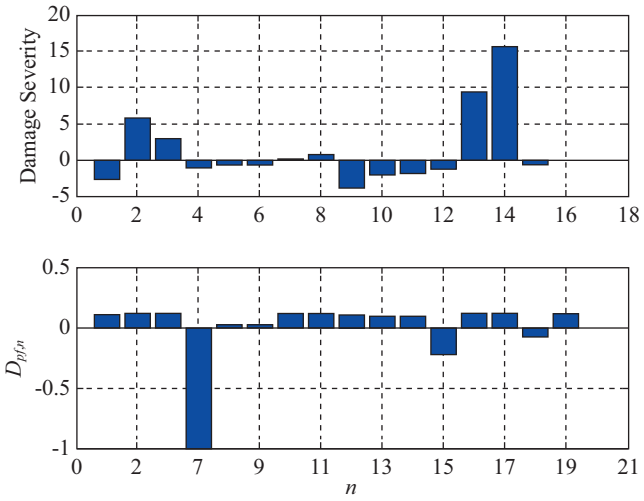

Fig. 10. Element 7 and Element 15 cut off simultaneously.

trated in Fig. 10 were obtained. This study concluded that elements 7, 15, and 18 were damaged before the second test was implemented; thus, the damage or damages that occurred after the first tests could not be determined.

When the proposed approach, which involves using the first and second measured data simultaneously, was implemented in the scenario (in which two measured modes were employed), the results shown in Fig. 11 were obtained. These results clearly indicated that damage at element 15 occurred between the first and second tests.

VI. CONCLUSION

Damage detection is generally extremely difficult when only a single platform measurement is used. This paper proposes a new damage evaluation method for identifying damages that occur between adjacent measurements. One

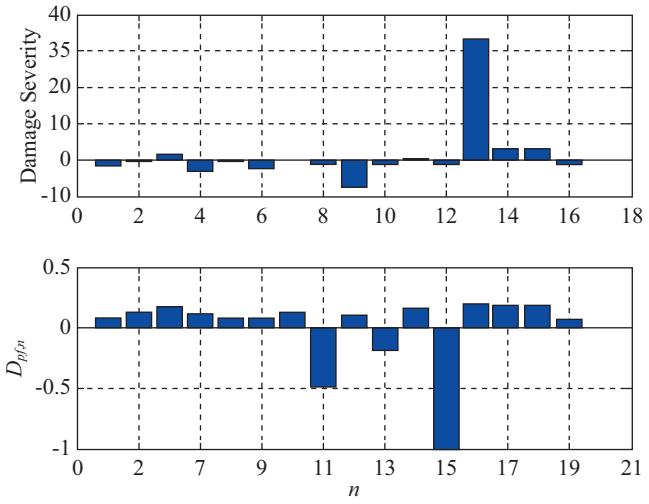

Fig. 11. Damage localization using the adjacent tests.

theoretical improvement is that the requirement of using the stiffness matrix of the FEM to replace that of the measured model can be ignored in calculating the MSE of the measured model. The other improvement is that the effects of the damages accumulated before the first measurement in the damage detection that occurs between the two measurements can be considerably reduced. The results of numerical studies also demonstrated that the proposed method can be used to localize the damages that occur in the time interval of two adjacent measurements and to evaluate these damages accurately, even in spatially incomplete situations. Furthermore, the experimental results clearly indicate that the damage at element 15 that occurred between the first and second test could be detected accurately.

ACKNOWLEDGMENTS

This research work is financially supported by the 973 project (Grant no. 2011CB013704) of the National Natural Science Foundation of China (Grant nos. 51279188, 51009124, 51379197, 51479184).

REFERENCES

1. Elshafey, A. A., Haddara, M. R., and Marzouk, H., "Damage detection in offshore structures using neural networks," *Marine Structures*, Vol. 23, No. 1, pp. 131-145 (2010).
2. Friswell, M. I., Inman, D. J., and Pilkey, D. F., "Direct updating of damping and stiffness matrices," *AIAA Journal*, Vol. 36, No. 3, pp. 491-493 (1998).
3. Li, H. J., Liu, F. S., and Hu, S.-L. J., "Employing incomplete complex modes for model updating and damage detection of damped structures," *Science in China Series E: Technological Sciences*, Vol. 51, No. 12, pp. 2254-2268 (2008).
4. Li, H. J., Yang, H. Z., and Hu, S.-L. J., "Modal strain energy decomposition method for damage localization in 3D frame structures," *Journal of Engineering Mechanics*, Vol. 132, No. 9, pp. 941-951 (2006).
5. Liu, F. S., "Direct mode-shape expansion of a spatially incomplete measured mode by a hybrid-vector modification," *Journal of Sound and Vibration*, Vol. 330, Nos. 18-19, pp. 4633-4645 (2011).
6. Liu, F. S., Chen, Z. S., and Li, W., "Non-iterative mode shape expansion for three-dimensional structures based on coordinate decomposition," *Journal of Vibroengineering*, Vol. 14, No. 3, pp. 984-993 (2012).
7. Liu, F. S. and Li, H. J., "Rapid direct mode shape expansion for offshore jacket structures using a hybrid vector," *Ocean Engineering*, Vol. 51, No. 1, pp. 119-128 (2012).
8. Liu, F. S. and Li, H. J., "A two-step mode shape expansion method for offshore jacket structures with physical meaningful modelling errors," *Ocean Engineering*, Vol. 63, No. 1, pp. 26-34 (2013).
9. Mangal, L., Idichandy, V. G., and Ganapathy, C., "ART-based multiple neural networks for monitoring offshore platforms," *Applied Ocean Research*, Vol. 18, Nos. 2-3, pp. 137-143 (1996).
10. Mojtahedi, A., Lotfollahi Yaghin, M. A., Hassanzadeh, Y., Ettefaghb, M. M., Aminfar, M. H., and Aghdam, A. B., "Developing a robust SHM method for offshore jacket platform using model updating and fuzzy logic system," *Applied Ocean Research*, Vol. 33, No. 4, pp. 398-411 (2011).
11. Shi, Z. Y., Law, S. S., and Zhang, L. M., "Structural damage localization from modal strain energy change," *Journal of Sound Vibration*, Vol. 218, No. 5, pp. 714-733 (1998).
12. Stubbs, N., Kim, J. T., and Farrar, C. R., "Field verification of a nondestructive damage localization and severity estimation algorithm," *Proceedings of the IMAC, Society of Experimental Mechanics*, Connecticut, USA, pp. 210-218 (1995).
13. Surace, C. and Worden, K., "A novelty detection method to diagnose damage in structures: an application to an offshore platform," *Proceedings of the Eighth International Offshore and Polar Engineering Conference*, Vol. 4, pp. 64-70 (1998).